

## Porous-structured Conductive Polypyrrole Cell Scaffolds

Joo-Woon Lee

Chemistry-School of Liberal Arts and Sciences, Korea National University of Transportation,  
Chungju, Chungbuk 380-702, Korea. E-mail: jwoonlee@ut.ac.kr

Received September 23, 2013, Accepted October 21, 2013

**Key Words :** Conductive polymer, Polypyrrole, Scaffold, Cell adhesion

As numerous cells favorably respond to electrical stimulation,<sup>1</sup> intrinsically conductive polymers (ICPs) have gained much attention for biomedical applications such as biosensors, tissue engineering scaffolds, and bioelectronic devices.<sup>2</sup> Among ICPs, polypyrrole (PPy) has evolved as a promising platform in biomedical area because of its inherent electroactive properties, biocompatibility, and ease of synthesis.<sup>3</sup>

Intensive efforts have been made to tailor PPy surfaces capable of improving cellular activity. The most common strategy is to physically entrap anionic biomolecules as dopants into the PPy during electrochemical polymerization.<sup>4</sup> Functional groups of the dopants were used to graft peptides or proteins to further enhance specific performance of the PPy. However, the PPy modified by the strategy above have exhibited decreased electrical conductivity and impaired mechanical properties. Since most of the expended dopants are incorporated into the bulk, it results in disruption of the film.<sup>5</sup> Another approach is to directly incorporate functionalities into the PPy backbone by polymerizing monomeric pyrrole derivatives with pendant functionalities, because conventional pyrrole monomer lacks reactive functional groups capable of covalently modifying PPy surfaces with biomolecules.<sup>6</sup> Despite the significant advancement in surface modification and utilization as bioactive interfaces, however, creation of pendant functionalities on the PPy backbone is complex and still remains challenging by reason of preserving intrinsic PPy bulk properties such as conductivity and mechanical and thermal integrity.

Recent research has been concentrated on micro-/nano-structured porous PPy scaffolds with high surface-to-volume ratio while retaining structural stability.<sup>2a,7</sup> This is because that the preservation of PPy's intrinsic electrical conductivity is a key advantage of the porous micro-/nanostructures over the any approaches<sup>4,6</sup> above. Numerous studies have also indicated that cell adhesion can be physically controlled by substrate topography.<sup>8</sup> To date, the porous micro-/nanostructures of PPy have been fabricated by electrochemical polymerization of PPy into templates composed of self-assembled multiple layers of poly(methyl methacrylate) colloids,<sup>9</sup> polystyrene nanospheres,<sup>10</sup> or mesoporous silica nanoparticles,<sup>11</sup> followed by subsequent removal of the templates. Therefore, such template-assisted fabrication of porous-structured PPy is one approach that can be applied to guide and enhance cellular behaviors. Herein agarose is

utilized for templating three-dimensionally porous-structured PPy scaffolds with cavities, pores, and interconnected channel networks, in an attempt to closely mimic the architecture of native extracellular matrix (ECM).

In the present study, electrically conductive PPy cell scaffolds were prepared by electropolymerization of PPy through the interstitial voids of a thermo-sensitive agarose hydrogel ( $T_{Gel} \sim 20^\circ\text{C}$ ) template. Selective removal of the template from the PPy-agarose matrix immersed into boiling water yielded porous-structured PPy scaffolds. Human umbilical vein endothelial cells (HUVECs) were seeded and cultured over the PPy scaffolds to quantify the cell viability. The PPy with high surface area and interconnected porous networks exhibited enhanced cell adhesion and proliferation compared to conventional non-porous PPy.

As schematically illustrated in Figure 1, porous-structured PPy films were successfully prepared by the electrochemical PPy deposition within a sacrificial agarose gel template and the subsequent selective removal of the template from the PPy-agarose matrix. Film thickness of the porous-structured PPy was measured to be *ca.* 200 nm and the electrical conductivity was measured to be *ca.*  $2.80\text{ S}\cdot\text{cm}^{-1}$ . In the course of PPy electropolymerization, the PPy has grown through the agarose gel template to near the top of the template, without actually covering over it. It is crucial in preparing the PPy-agarose matrix for PPy not to grow completely

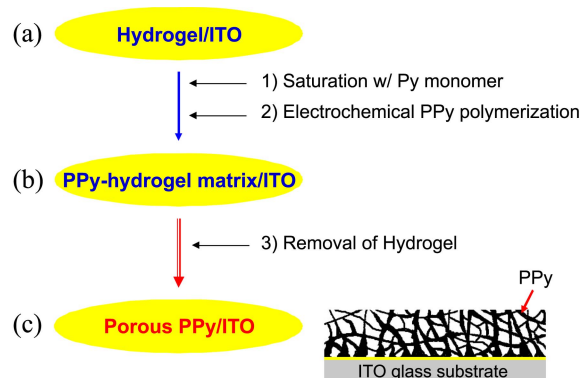


**Figure 1.** Schematic illustration of porous-structured PPy scaffold preparation: (a) sacrificial hydrogel template on ITO substrate and the electrochemical polymerization of PPy through the interstitial voids in the hydrogel template, (b) selective removal of hydrogel template from PPy-hydrogel matrix, and (c) PPy scaffold with three-dimensional porosity.

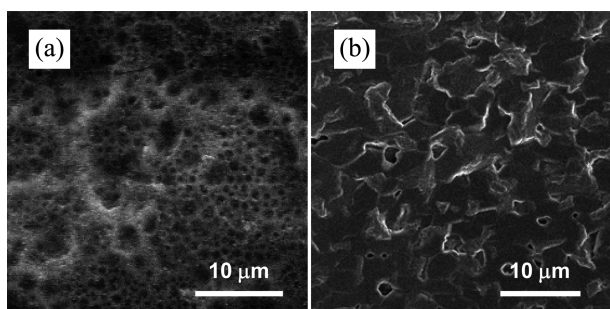


**Figure 2.** Scanning electron micrographs of (a) porous-structured PPY films and (b) conventional non-porous PPY films.

through the agarose template and to form a non-porous layer over the template. Figure 2(a) presents a typical scanning electron micrograph of the PPY films with three-dimensionally porous structures, compared to that of conventional non-porous electrodeposited PPY films in Figure 2(b). Polymerization procedures for conventional films matched those for porous-structured PPY films except that no agarose hydrogel was used as a template. Three-dimensional porosity of the PPY cell scaffolds provides increased surface area and hollow micro-/nanostructures, which may facilitate cell distribution when cells are seeded with media over the cell scaffolds.

Chemical composition (in atomic %) at the surface of the porous-structured PPY was determined using X-ray photoelectron spectrometer (XPS). No foreign elements beyond C(1s), N(1s), O(1s), Cl(2s), and Cl(2p) were detected in the survey spectrum (not shown), so no adjustment was made in the analysis. The doping level was calculated to be *ca.* 25.2% from high-resolution (HR) Cl(2p)/N(1s) ratio, and deconvolution of the HR N(1s) provides the relative ratio ( $I_{N^+}/I_{N_{tot}}$ ) of the oxidized nitrogen fractions (C-N<sup>+</sup> and C=N<sup>+</sup>) to be 24.9% in Figure 3, which is quantitatively relevant to the former doping level calculation.

To demonstrate the potential to influence cellular activity,

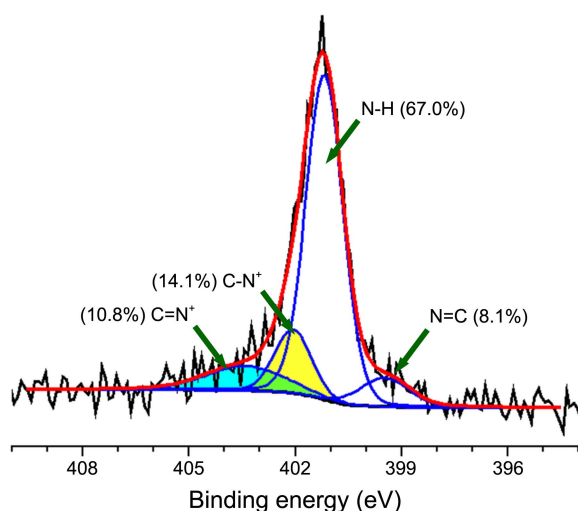


**Figure 3.** Deconvolution of high-resolution XPS spectrum relevant to N(1s) envelope of porous-structured PPY films. The spectrum contains four fractions based on the chemical bonds.

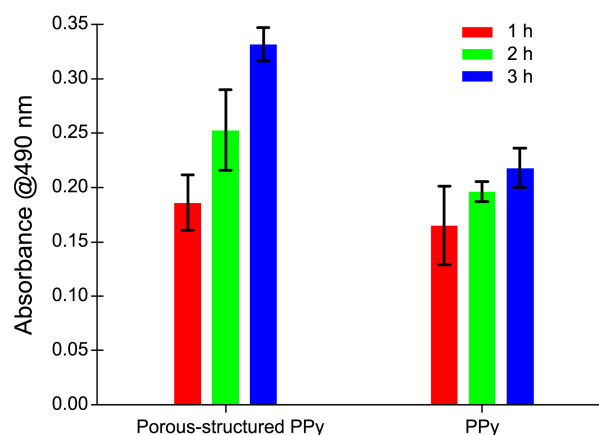


**Figure 4.** Viability of human umbilical vein endothelial cells (HUVECs) measured on the porous-structured PPY films and on a negative control conventional PPY as a function of incubation time using an MTS cell proliferation assay. For all samples,  $n = 3-5$ , and typically  $n = 3$ . Error bars represent the standard deviation.

HUVECs were seeded and cultured on the porous-structured PPY and the extent of the cell adhesion was quantitatively evaluated using an MTS cell proliferation assay.<sup>12</sup> A negative control conventional PPY film also underwent identical cell-seeding procedure to compare the effect of topographical features. The data in Figure 4 represent average absorbance values at 490 nm of the formazan product derived from the reduction of MTS, and the error bars reflect the standard error of the mean at each incubation time point. The results indicate that the porous-structured PPY increased the viability of HUVECs compared to the control conventional PPY: the absorbance at 3 h time point for the PPY with porosity ( $0.332 \pm 0.015$ ;  $n = 3$ ) was 50% higher than for the negative control ( $0.218 \pm 0.018$ ;  $n = 3$ ), which was statistically significant for comparison ( $p < 0.01$ ). The results suggest that the increased surface area and three-dimensionally hollow micro-/nanostructures can contribute to promoting cell adhesion and proliferation.

In conclusion, three-dimensionally porous-structured PPY cell scaffolds are fabricated by electrochemical polymerization of PPY through the interstitial voids of a thermo-sensitive agarose gel template and the subsequent selective removal of the template from the PPY-agarose matrix. The developed topographical features led to the enhanced cell adhesion and proliferation of HUVECs compared to that of a negative control conventional PPY. The higher viability of HUVECs on the porous-structured PPY can be attributed to the increased surface area and three-dimensionally hollow micro-/nanostructures, which can facilitate cell distribution and adhesion. This simple physical approach can be further exploitable for developing bioactive conducting cell scaffolds, by integrating chemical approaches to incorporate functionalities into a new strategy.

## Experimental Section

**Materials.** Agarose (Type IX-A, Sigma), hydrochloric acid

(HClO<sub>4</sub>, Aldrich), human umbilical vascular endothelial cells (HUVECs, Cambrex), endothelial cell medium-ECM (Cambrex), and MTS reagent (Promega) were used as received; however, pyrrole (Sigma) monomer was distilled and stored at -20 °C under argon until use. Indium tin oxide (ITO) conductive borosilicate glass slides with typical resistance of 30-60 Ω (Delta Technologies, Ltd.) were sequentially cleaned in acetone, methanol, isopropyl alcohol, and distilled deionized (DDI) water for 5 min each with ultrasonication. Slides were then dipped in a 1.0 N NaOH solution for 30 min, washed with copious amounts of DDI water, and dried under vacuum.

**Preparation of Porous-structured PPy Scaffolds.** Figure 1 schematically depicts the hydrogel template procedure used for the preparation of porous-structured PPy films.

Pyrrole precursor solution was prepared by adding HClO<sub>4</sub> (1.0 M) to pyrrole (0.5 M) aqueous solution in 2:1 molar ratio and the solution was then deoxygenated at ambient temperature (~20 °C) with argon (Ar) for 10 min to prevent oxidation of the monomers. While agarose was added to DDI water at 20 mg/mL, heated to over 90 °C until completely dissolved, and allowed to cool to 50-55 °C. 500 μL of the agarose solution was then cast onto a 2.54 × 2.54 cm<sup>2</sup> ITO glass slide which was pre-warmed to 50-55 °C and allowed to cool to ambient temperature to form gel.<sup>13</sup> The obtained agarose gel served as templates for subsequent fabrication of porous-structured PPy.

The agarose gel on ITO slides was subsequently dipped into the pyrrole precursor solution for 24 h so as to soak through the entire gel and was saturated with the same concentration of the outer pyrrole solution. Electropolymerization of the pyrrole through the interstitial voids of the agarose gel template was carried out using a potentiostat/galvanostat (KST-P1, KOSENTECH) with a three-electrode electrochemical set up. The agarose gel template on ITO slide was used as the working electrode, a platinum mesh was served as a counter electrode, and a saturated calomel electrode served as a reference electrode. PPy films were deposited at an offset voltage of 720 mV in the pyrrole precursor solution. The film thickness was monitored and controlled by integrating the passage of current.

To remove the template, the PPy-agarose matrix on the ITO was then immersed into DDI water, which was heated to over 90 °C for overnight to selectively dissolve agarose out from the matrix. The resulting porous-structured PPy films were finally rinsed with copious amount of hot DDI water and dried at ambient temperature.

**Characterization.** Chemical composition of the polymer surfaces was determined using a Physical Electronics (PHI) 5700 XPS equipped with an Al monochromatic source (Al KR energy of 1486.6 eV) and a hemispherical analyzer. The energy resolution was 1.0 eV for survey spectra and 0.1 eV for HR spectra. Binding energies were calibrated by setting the C-C/C-H<sub>x</sub> component in the C(1s) envelope at 284.6 eV. The doping level was determined from the Cl/N ratio of HR Cl(2p) and N(1s) core-level XPS spectra. Conductivity at ambient temperature was measured with a conventional

four-point probe resistivity apparatus placed on the polymer films. Film thickness was measured using a profilometer (Alpha Step 200, Tencor Instruments) and surface morphology was examined using scanning electron microscopy (SEM) (S-4000, Hitachi).

**Cell Adhesion and Viability.** Cell adhesion studies were performed to validate the improved bioactivity of the porous-structured PPy. HUVECs were seeded in 1.5 cm<sup>2</sup> wells with 1 mL of ECM media at a density of 30 000 cells/cm<sup>2</sup> and cultured for 1 h in the absence of serum on the porous-structured films and a negative control conventional PPy. The colorimetric MTS cell proliferation assay was performed to quantify the extent of cell adhesion. Following 1 h of incubation in serum-free media, surfaces were rinsed three times by gently shearing 1 mL of 10 mM PBS over the film surface to remove unattached and loosely attached cells. PBS was aspirated, and new medium containing 2% fetal bovine serum (FBS) and 20% MTS reagent was added to each well and allowed to incubate at 37 °C for 1, 2, and 3 h time points. Cell viability was evaluated by removing 100 μL of media from the wells and measuring the absorbance of media at 490 nm using a microplate reader (Synergy<sup>TM</sup> HT, BioTek). At least three samples were averaged to calculate each time point.

**Acknowledgments.** The research was supported by a grant from the Academic Research Program of Korea National University of Transportation in 2013.

## References

- (a) Basset, C. A.; Pawluk, R. J.; Becker, R. O. *Nature* **1964**, *204*, 652. (b) Kerns, J. M.; Pavkovic, I. M.; Fakhouri, A. J.; Wickersham, K. L.; Freeman, J. A. *J. Neurosci. Methods* **1987**, *19*, 217. (c) Wong, J. Y.; Langer, R.; Ingber, D. E. *Proc. Natl. Acad. Sci. USA* **1994**, *91*, 3201. (d) Aoki, T.; Tanino, M.; Sanui, K.; Ogata, N.; Kumakura, K. *Biomaterials* **1996**, *17*, 1971.
- (a) Guimard, N. K.; Gomez, N.; Schmidt, C. E. *Prog. Polym. Sci.* **2007**, *32*, 876. (b) Cui, X.; Wiler, J.; Dzaman, M.; Altschuler, R.; Martin, D. C. *Biomaterials* **2003**, *24*, 777. (c) Geetha, S.; Chepuri, R. K.; Rao, M.; Trivedi, D. C. *Anal. Chim. Acta* **2006**, *568*, 119. (d) Kim, D.; Abidian, M.; Martin, D. C. *J. Biomed. Mater. Res. A* **2004**, *71*, 577. (e) Yang, J.; Martin, D. C. *Sens. Actuators B* **2004**, *101*, 133.
- (a) Laleh, G. M.; Molamma, P. P.; Mohammad, M.; Mohammad, H. N. E.; Hossein, B.; Sahar, K.; Salem, S. A. I. D.; Seeram, R. *J. Tissue Eng. Regen. Med.* **2011**, *5*, 17. (b) Green, R. A.; Lovell, N. H.; Poole-Warren, L. A. *Acta Biomater.* **2010**, *6*, 63. (c) George, P. M.; Lyckman, A. W.; LaVan, D. A.; Hegde, A.; Leung, Y.; Avasare, R.; Testa, C.; Alexander, P. M.; Langer, R.; Sur, M. *Biomaterials* **2005**, *26*, 3511-3519.
- (a) Kim, D. H.; Richardson-Burns, S. M.; Hendricks, J. L.; Sequera, C.; Martin, D. C. *Adv. Funct. Mater.* **2007**, *17*, 79. (b) Green, R. A.; Lovell, N. H.; Poole-Warren, L. A. *Acta Biomater.* **2010**, *6*, 63. (c) Liu, X.; Yue, Z.; Higgins, M. J.; Wallace, G. G. *Biomaterials* **2011**, *32*, 7309. (d) Song, H.-K.; Toste, B.; Ahmann, K.; Hoffman-Kim, D.; Palmore, G. T. R. *Biomaterials* **2006**, *27*, 473.
- Green, R. A.; Lovell, N. H.; Poole-Warren, L. A. *Biomaterials* **2009**, *30*, 3637.
- (a) Lee, J.-W.; Serna, F.; Nickels, J.; Schmidt, C. E. *Biomacromolecules* **2006**, *7*, 1692. (b) Lee, J. W.; Serna, F.; Schmidt, C. E. *Langmuir* **2006**, *22*, 9816. (c) Lee, J. Y.; Lee, J.-W.; Schmidt, C.

- E. *J. R. Soc. Interface* **2009**, *6*, 735. (d) Cho, Y.; Borgens, R. B. *Nanotechnology* **2010**, *21*, 205102/1.
7. Eftekhari, A. *Nanostructured Conductive Polymers*; Wiley: Chichester, U. K., 2010.
8. (a) Miller, C.; Jeftinija, S.; Mallapragada, S. *Tissue. Eng.* **2002**, *8*(3), 367. (b) Rajnicek, A.; Britland, S.; McCaig, C. *J. Cell Sci.* **1997**, *110*(Part 23), 2905. (c) Stokols, S.; Tuszynski, M. H. *Bio-materials* **2006**, *27*, 443.
9. Sharma, M.; Waterhouse, G. I. N.; Loader, S. W. C.; Garg, S.; Svirskis, D. *Int. J. Pharm.* **2013**, *443*, 163.
10. (a) Kang, G.; Borgens, R. B.; Cho, Y. *Langmuir* **2011**, *27*, 6179. (b) Pokki, J.; Ergeneman, O.; Sivaraman, K. M.; Özkale, B.; Zeeshan, M. A.; Lüthmann, T.; Nelson, B. J.; Pané, S. *Nanoscale* **2012**, *4*(10), 3083.
11. Cho, Y.; Borgens, R. B. *Nanotechnology* **2010**, *21*, 205102.
12. Barltrop, J. A.; Owen, T. C.; Cory, A. H.; Cory, J. G. *Bioorg. Med. Chem. Lett.* **1991**, *1*, 611.
13. Andrews, A. T. *Electrophoresis: Theory, Techniques, and Biochemical and Clinical Applications*, 2nd ed.; Clarendon Press: Oxford, U. K., 1993; p 149.
-